Radiation Protection Considerations for the Cryogenic In-Vacuum Undulator of the EMIL Project at BESSY

Y. Bergmann and K. Ott

Helmholtz-Zentrum Berlin, BESSYII, Albert-Einstein-Str. 15, 12489 Berlin, Germany

Abstract

The Helmholtz-Zentrum Berlin and the Max Planck Society will implement a new dedicated X-ray beamline at the synchrotron light source BESSY II for the analysis of materials for the regenerative energy generation. The project is called EMIL, the Energy Materials In-Situ Laboratory Berlin, [1] and the beamlines had to deliver x-rays with a needed energy range from 80 eV up to 12000 eV. Therefore two undulators will be placed in a single straight section, for soft x-rays an elliptical APPLE II device and for hard x-rays a cryogenic in-vacuum undulator.
To determine adequate measures of the shielding of synchrotron radiation in the experimental hall we use the particle transport code FLUKA [2] [3]. We calculated the synchrotron radiation spectra for the cryogenic undulator with the code SPECTRA10 [4]. After modeling the modified section of the storage ring and the new beamlines we determined the thickness of the shielding walls of the hutches with the results of spectra sampling with FLUKA up to 30000 eV. The APPLE II undulator does not have to be considered for the hutch design because of its low energy synchrotron radiation (80 eV up to 2000 eV) which is absorbed in the vacuum system.
Additionally we considered the effects of the bremsstrahlung with FLUKA simulations.

1. Introduction

The 1.7 GeV storage ring BESSY II with a circumference of 240 m started its operation in 1998 and now supplies 52 beamlines with synchrotron radiation. It is divided into 16 sections whereof 14 sections are filled with undulators, wigglers and super conducting insertion devices. The residual sections are used for the cavities and injection septum. Since 2012 BESSY II is operating in top-up mode [5].
At this storage ring a new project was implemented, the Energy Materials In-Situ Laboratory (EMIL). Therefore the HZB and MPG combine their competences to build this new facility on material and process development. Several beamlines will be implemented within sum five end stations. One end station is called SISSY and is designed for the investigation of photovoltaic devices and materials under in-system conditions of the fabrication process. Another new end station is CAT where (photo) catalytic materials and processes under ambient conditions can be studied with spectroscopic methods. The large variety of the available methods in the end stations requires a bright energy range of the delivered x-rays from 80 eV up to 12000 eV. Two undulators will be implemented as new light source for EMIL. Responsible for the soft x-rays is an APPLE II type undulator and the hard x-rays will be realized by a cryogenic undulator. Two independent beamlines supply the measuring stations with the x-rays, so it is possible to use both beams or separate one. To realize this project more than 20 optical elements like mirrors, gratings and crystals have to be installed. To reach the end stations the beam has to pass an overall distance of 60 m in a small corridor of less than 1 m. The existing experimental hall is not only traversed by the new beamlines, it will be complemented by two new experimental setups. Therefore we have to deal with the question of required safety measures inside the experimental hall. The high intensity of synchrotron radiation requires a high accuracy in shielding and safety design for the beamlines.

2. Insertion Device and Beamline

Two canted undulators supply the new beamlines with synchrotron radiation [6]. Both undulators will be installed in the same low-β section at the BESSY II storage ring. For a reasonable separation of the beam cones and some safety margin a canting angle of two mrad was selected.
To cover the soft x-ray regime from 80 eV up to 2000 eV an elliptical APPLE II device (UE-48, *Figure 1*) with a period of 48 mm and 29 periods is utilized. The magnets of this undulator consist of neodymium iron boron (one A- and one B- magnet) and were magnetized in a 45° oriented magnetic field.
The vacuum chamber of this device is made of an extruded Aluminum with an elliptical inner cross section where the inner surface is coated with non-evaporable getter (NEG).

For the hard x-ray regime, up to 12000 eV, an in-house developed cryogenic in-vacuum undulator (U-17, *Figure 1*) with a period length of 17 mm and 88 periods will be used. The undulator is based on cryogenically cooled $(Pr,Nd)_2Fe_{14}B$ magnets. Some parameters of the two undulators like the minimum magnetic gap are shown in *Table 1*.

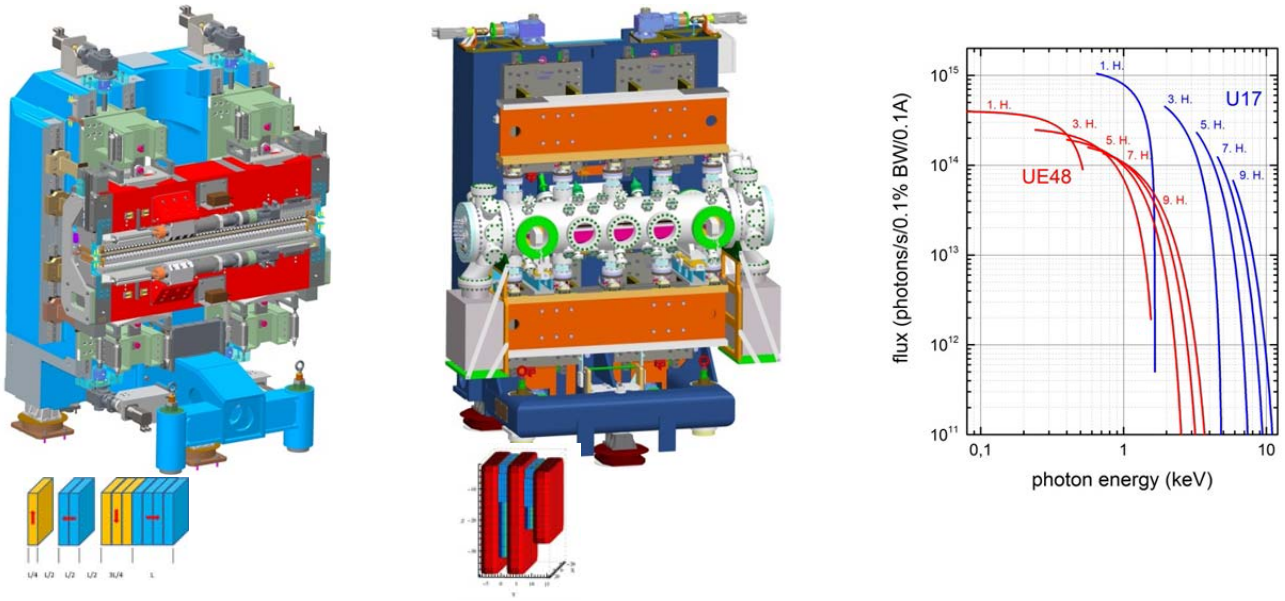

Figure 1 *- Layout and End-pole configuration of both undulators and Photon Flux*

UNDULATOR	**UE-48**	**U-17**
Period length	48 mm	17 mm
Periods	31	88
K	3,4	1,78
Gap_{min}	15 mm	5,5 mm
Total Power (300mA)	479 W	1031 W

Table 1 *- Parameter of the soft and hard x-ray light source UE-48 and U-17*

The synchrotron radiation generated by the normal conducting UE-48 will be absorbed in the 2 mm stainless steel of the beamline vacuum system because of its critical energy which is below 2.5 keV. With regard to the shielding design there is no necessity to consider the beam emitted by the UE-48 with the exception of thinner materials like bellows or windows which are additionally shielded by lead.
In respect to the energy range the synchrotron radiation of the U-17 will not be absorbed in the vacuum system. The beamline of this super conducting insertion device has to be positioned in hutches. To design the shielding measures of the hutches as accurately as possible the calculation of the spectrum of the U-17 is essential and presented in the following. For beamline shielding with the calculated spectrum we used the FLUKA Monte Carlo simulation code.
The EMIL beamline delivers three experimental endstations inside the EMIL facility. There are two endstations within the experimental hall: on the one hand the PEEM (photo emission electron microscopy) supplied with the soft branch and on the other hand the Pink station supplied with the hard branch. Each station is enclosed with its own experimental hutch.
An overview of the EMIL beamline [7] with the optical elements like mirrors and crystals and the undulators is shown in *Figure 2* as well as the schematic representation of the different hutches.
The generated beam first has to pass several mirror chambers inside the ring tunnel where the synchrotron radiation is separated from the bremsstrahlung. With the included absorbers the bremsstrahlung will be kept within the ring tunnel and the deflected synchrotron radiation will enter the optical components placed within the optics hutch close to the shielding wall. The monochromators are located in the optics hutch and are used for the beamline of PEEM and the EMIL Lab.

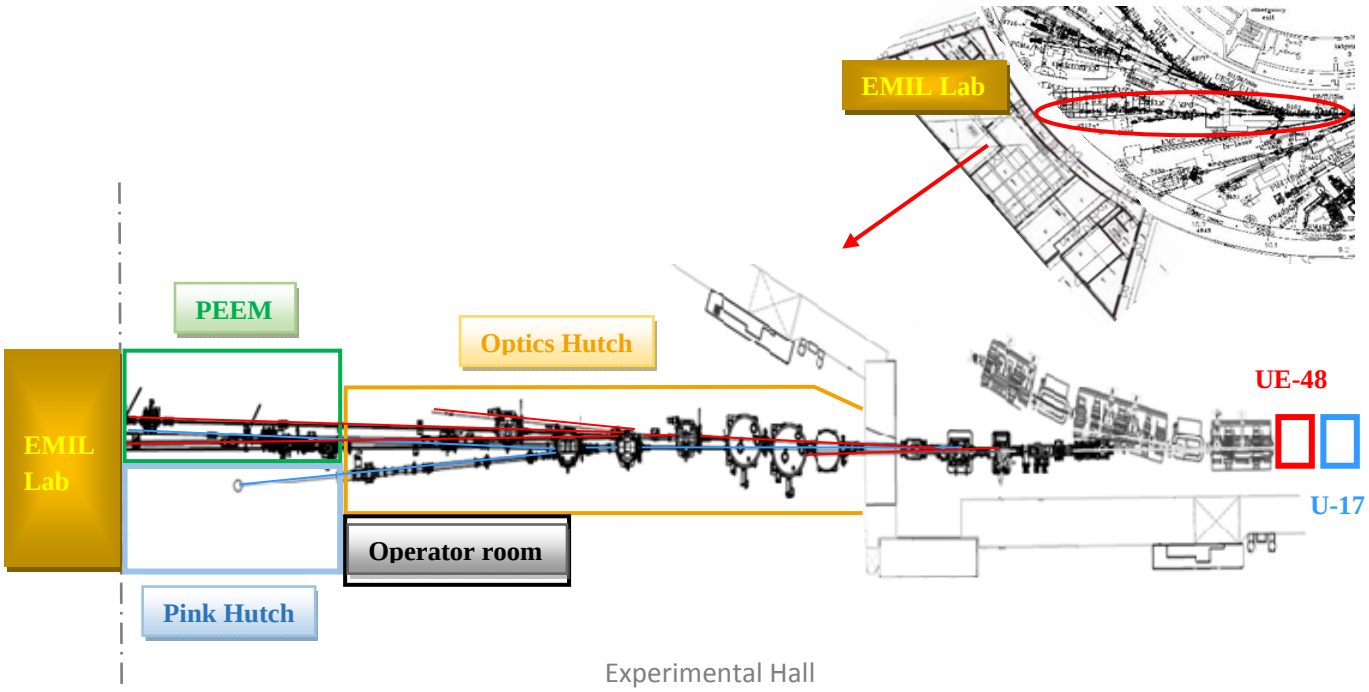

Figure 2 - *Overview of the EMIL beamline with the several hutches and optical path of soft (red) and hard (blue) x-rays*

3. Calculation of Synchrotron Radiation

In the following we give an overview how synchrotron spectra could be calculated from first principles.

3.1. Basic Considerations

The scalar and vector potentials of a moving charge are given by the Liénard – Wiechert potentials:

$$V(t) = \frac{e}{4\pi\varepsilon_0}\left\{\frac{1}{r(1-\vec{n}\cdot\vec{\beta})}\right\}_{ret}$$
$$\vec{A}(t) = \frac{\mu_0 e}{4\pi}\left\{\frac{\vec{\beta}c}{r(1-\vec{n}\cdot\vec{\beta})}\right\}_{ret} \qquad (1)$$

The expressions in the brackets have to be calculated for the time of emission (the retarded time), the potentials are given for the time of observation. *n* is the vector pointing from the charge to the observer at the retarded time, *r* is the respective distance, β is the normalized velocity. The electric and magnetic fields we get with

$$\vec{E} = -\vec{\nabla}V - \frac{\partial\vec{A}}{\partial t} \text{ and } \vec{B} = \vec{\nabla}\times\vec{A} \qquad (2)$$

resulting in the Liénard – Wiechert equations [8].

$$\vec{E}(t) = \frac{e}{4\pi\varepsilon_0}\left\{\frac{(1-\beta^2)(\vec{n}-\vec{\beta})}{r^2(1-\vec{n}\cdot\vec{\beta})^3} + \frac{\vec{n}\times((\vec{n}-\vec{\beta})\times\dot{\vec{\beta}})}{cr(1-\vec{n}\cdot\vec{\beta})^3}\right\}_{ret}$$
$$\vec{B}(t) = \frac{\vec{n}_{ret}\times\vec{E}}{c} \qquad (3)$$

The electric field consists of two terms, the first one is proportional to $1/r^2$ and does not require an accelerated charge. The second one is proportional to $1/r$ and describes the result of acceleration.

In the so called far field approximation, which is appropriate for the production of synchrotron radiation, only the second term is used.

We consider now a coordinate frame which is longitudinal moving with the charge and the transversal movements of this charge (betatron oscillations, undulators) leads to electric dipole radiation.
No radiation is emitted in the direction of the transversal motion.
With the relativistic longitudinal velocities that are common at synchrotron light sources this dipole radiation is Lorentz - transformed to the laboratory frame in a forward directed cone with a small opening angle of $1/\gamma$.
The power density (in W/m²) emitted by the moving charge is given by the Poynting vector:

$$\vec{S} = \frac{1}{\mu_0}(\vec{E} \times \vec{B}) = \frac{1}{\mu_0 c}(\vec{E} \times (\vec{n}_{ret} \times \vec{E})) = \frac{1}{\mu_0 c}(E^2\vec{n} - (\vec{n} \cdot \vec{E})\vec{E}) \tag{4}$$

The Poynting vector gives the directional energy flow per unit time *t* through a unit area. The irradiated power seen by the observer at time *t* for transversal acceleration (n is normal to E) is:

$$\frac{dP}{d\Omega} = r^2\left|\vec{S}\right| = \frac{E^2}{\mu_0 c} \tag{5}$$

3.2. Synchrotron Radiation Spectra

To get the power spectrum we calculate the Fourier transformation of the electric field equation (3). In the general expression

$$\tilde{E}(\omega) = \frac{1}{\sqrt{2\pi}}\int_{-\infty}^{+\infty} E(t)e^{-i\omega t}dt \tag{6}$$

In the Liénard - Wiechert eq. (3) the retarded time is used. So we have to substitute the time *t* by the retarded time *t´* with the expressions

$$t = t' + \frac{r(t')}{c}\,;\; dt = (1 - \vec{n} \cdot \vec{\beta})dt' \tag{7}$$

Inserting the electric field eq. of (3) in (6) we get with (7)

$$\tilde{E}(\omega) = \frac{e}{4\pi\varepsilon_0 c}\frac{1}{\sqrt{2\pi}}\int_{-\infty}^{+\infty}\left(\frac{\vec{n} \times ((\vec{n} - \vec{\beta}) \times \dot{\vec{\beta}})}{r(1 - \vec{n} \cdot \vec{\beta})^2}\right)e^{-i\omega(t' + r(t')/c)}dt' \tag{8}$$

Eq. (8) contains already the far field approximation of (3), only the field contribution of the accelerated charge is considered. A further simplification is possible, if we consider the velocity of the charge as relativistic ($\gamma >> 1$). In that case the trajectory of the particle is Lorentz contracted (ρ/γ), the distance to the observer is much larger than the curvature. The vectors n und r change slowly during the radiation flash and are therefore kept constant (not in the exponential). In that case a partial integration is possible leading to the frequency dependent form of the Liénard – Wiechert equations. The magnetic field eq. (3) remains unchanged.

$$\tilde{\tilde{E}}(\omega) = \frac{i\omega e}{4\pi\varepsilon_0 c r_p\sqrt{2\pi}}\int_{-\infty}^{+\infty}(\vec{n} \times (\vec{n} \times \vec{\beta}))e^{-i\omega(t' + r(t')/c)}dt' \tag{9}$$

The energy *U* that a single particle irradiates by passing a curved trajectory can be calculated by time integrating the power (5). For the time – dependent electric field the expression for the inverse Fourier transform is used, which is the integral over the frequency - dependent electric field (9). We get then the angular spectral energy distribution

$$\frac{d^2U}{d\Omega d\omega} = \frac{2r^2\left|\tilde{\vec{E}}(\omega)\right|^2}{\mu_0 c} \tag{10}$$

If we consider a circular orbit with the radiation emitted as a short flash we can calculate the average spectral angular power density just by dividing this expression through the convolution time or by multiplying it with the convolution frequency. So we get

$$\frac{d^2P}{d\Omega d\omega} = \frac{\omega_0}{2\pi}\frac{d^2U}{d\Omega d\omega} = \frac{\omega_0 2r^2\left|\tilde{\vec{E}}(\omega)\right|^2}{2\pi\mu_0 c} \tag{11}$$

3.3. Application for Undulators

For an undulator with the length $L_u = N_u \lambda_u$, the wave number $k_u = \lambda_u / (2\pi)$, and the vertical field component $B_y = B_0 \cos(k_u z)$, we get from the Lorentz force two differential equations for the transversal and longitudinal motion:

$$\ddot{x} = -\frac{eB_0}{m_0\gamma}\cos(k_u z)\dot{z}; \quad \ddot{z} = \frac{eB_0}{m_0\gamma}\cos(k_u z)\dot{x} \tag{12}$$

Integrating the first equation und using

$$\dot{x}^2 + \dot{z}^2 = \beta^2 c^2 \tag{13}$$

we get the transversal and longitudinal velocities

$$\dot{x} = -\frac{cK_u}{\gamma}\cos(k_u z)\dot{z}; \quad \dot{z} = \beta c\sqrt{1-\frac{K_u^2}{\beta^2\gamma^2}\sin^2(k_u z)} \tag{14}$$

Here we used the undulator parameter K_u which is defined as the quotient of the maximal angle of the trajectory relative to the z – axis and the natural radiation opening angle $1/\gamma$ of the synchrotron radiation:

$$K_u = \gamma\psi = \frac{eB_0}{m_0 c k_u} \tag{15}$$

For normal undulators $K_u << 1$, and if $K_u > 1$ the undulator is considered as strong. For higher values the synchrotron radiation produced in the insertion device has a non – constructive interference and the insertion device is considered as wiggler. If the relativistic factor γ is large and $K_u << 1$ then the transversal velocity is non-relativistic. The longitudinal velocity is nearly unchanged in this case. For higher K_u values the average drift velocity through the undulator is smaller than the velocity of the particle.
In a frame moving with the drift velocity the motion in the weak undulator case is just a transversal motion. The resulting dipole radiation is monoenergetic. The frequency of the periodic particle motion is

$$\Omega_u = k_u \beta c \tag{15}$$

and increased by the Lorentz factor due to the Lorentz contraction of the undulator in the moving frame (signed with *). This frequency $\gamma\Omega_u$ is also the first harmonic ω_1 of the synchrotron radiation observed in the laboratory frame on the beam axis. The amplitude of the oscillation is the same in both frames. After elimination of the time dependence the relation of both coordinates in the moving frame is given by

$$z^* = \frac{aK_u}{4\beta}\frac{x^*}{a}\sqrt{1-\frac{x^{*2}}{a^2}}; \quad a = \frac{K_u}{\beta\gamma\ k_u} \tag{16}$$

For strong undulators the trajectory z*(x*) has the form of an ‘eight’.

In our case the undulator parameter of the U-17 is K_u =1.78 so we give an overview to get the power spectrum for a strong undulator. From eqs (12) und (14) we get the velocities and acclerations that we insert in the generalized form in the Liénard – Wiechert equation (1). Using the approximation for the far field and the high relativistic case we conduct the Fourier transformation for each harmonic

$$\frac{d^2P_m}{d\Omega d\omega} = \frac{2r^2\left|\tilde{\tilde{E}}_m(\omega)\right|^2}{\mu_0 L_u} \tag{17}$$

and the total radiation as the sum over all harmonics

$$\frac{d^2P}{d\Omega d\omega} = \sum_{m=1}^{\infty}\frac{d^2P_m}{d\Omega d\omega} \tag{18}$$

The calculations are straight forward but quite lengthy, so we present just the result [8]

$$\frac{d^2P_m}{d\Omega d\omega} = \frac{dP_m}{d\Omega} f_N(\Delta\omega_m) = P_u\gamma^{*2}\left[F_{m\sigma}(\theta,\phi) + F_{m\pi}(\theta,\phi)\right]f_N(\Delta\omega_m) \tag{19}$$

P_u is the average power emitted by one electron in an undulator

$$P_u = \frac{r_0 c m_0 c^2 k_u^2 K_u^2 \gamma^2}{3} \tag{19a}$$

For the strong undulator in eq. (19) the longitudinal velocity of the moving frame is close to c but somewhat lower than the velocity of the charge. This is related to the relativistic factor γ*, β* and K_u*.
The relations are

$$\gamma^* = \frac{1}{\sqrt{1-\beta^{*2}}} \approx \frac{\gamma}{\sqrt{1+K_u^2/2}}; \quad \beta^* = \beta\left(1-\frac{K_u^2}{4\beta^2\gamma^2}\right) \approx \beta; \quad K_u{}^* = \frac{K_u}{\sqrt{1+K_u^2/2}} \tag{19b}$$

In our case K_u* = 1.11 for K_u=1.78. The normalized angular distribution functions for the σ - mode (irradiation in the plane normal to the magnetic field) and the π - mode (irradiation parallel to the magnetic field) are

$$F_{m\sigma}(\theta,\phi) = \frac{3m^2}{\pi(1+K_u^2/2)^2 K_u{}^{*2}} \frac{(2\Sigma_{m1}\gamma^*\theta\cos\phi - \Sigma_{m2}K_u^2)^2}{(1+\gamma^{*2}\,\theta^2)^3}$$

$$F_{m\pi}(\theta,\phi) = \frac{3m^2}{\pi(1+K_u^2/2)^2 K_u{}^{*2}} \frac{(2\Sigma_{m1}\gamma^*\theta\sin\phi)^2}{(1+\gamma^{*2}\,\theta^2)^3} \tag{19c}$$

The sums are defined as

$$\Sigma_{m1} = \sum_{l=-\infty}^{\infty} J_l(ma_u) J_{m+2l}(mb_u)$$

$$\Sigma_{m2} = \sum_{l=-\infty}^{\infty} J_l(ma_u)(J_{m+2l+1}(mb_u) + J_{m+2l-1}(mb_u)) \tag{19d}$$

with the J as Bessel functions. The parameters a_u and b_u are

$$a_u = \frac{K_u^{*2}}{4(1+\gamma^{*2}\,\theta^2)}; \quad b_u = \frac{K_u^{*2}\gamma^*\theta\cos\phi}{1+\gamma^{*2}\,\theta^2} \tag{19e}$$

The normalized spectral function f_N is

$$f_N(\Delta\omega_m) = \frac{N_u}{\omega_1}\left(\frac{\sin\left(\frac{\Delta\omega_m \pi N_u}{\omega_1}\right)}{\left(\frac{\Delta\omega_m \pi N_u}{\omega_1}\right)}\right);\quad \omega_m = m\omega_1 = \frac{m2\gamma^{*2}\,\Omega_u}{1+\gamma^{*2}\,\theta^2};\quad \frac{\Delta\omega_m}{\omega_1} = \frac{\omega - m\omega_1}{\omega_1} \tag{19f}$$

3.4. Emission of Photons

So far we considered the production of synchrotron radiation in the frame of classical electrodynamics, as emission of electromagnetic waves. Synchrotron radiation is emitted as photons though, so we consider the storage ring as a macroscopic atom with huge quantum numbers. The photons have the energy

$$E_\gamma = \hbar\omega \tag{20}$$

To get the energy distribution of the emitted photon intensity, we divide the power by the photon energy

$$\frac{d^2P}{d\Omega d\omega}\cdot\frac{1}{\hbar\omega} = \frac{d^2\dot{n}}{d\Omega d\omega};\quad or\quad \frac{d^2P}{d\Omega d\omega} = \hbar\cdot\frac{d^2\dot{n}}{d\Omega d\omega/\omega} \tag{21}$$

As an important result we see the photon intensity for a *relative* frequency (or energy) bin is proportional to the power spectrum for a fixed frequency (or energy) bin. The widths of the relative bins grow with the energy, but with the same factor the energy width of the emitted photons. For a fixed binning the emission of the photon would be counted in many bins to calculate the likelihood for the emission of a photon of a given energy if a spectrum is used.
For the relative bins the 0.1 % bandwidth is quite common in that case dω/ω is replaced by Δω/ω (without integrating over ω) and finally replaced by 1E-3.

4. Spectrum Sampling with FLUKA

4.1. SPECTRA 10

In section 3 the analytical formula for the power spectrum of a strong undulator was given. Considerable simplifications of this formula are possible and shown in textbooks e.g. [9]. For example the geometric limitations vertical angle θ=0 and a small horizontal angle makes it possible not to include the contribution of the π - mode eq. (19c) and the even summands eq. (19c, 19d). In our case the usage of simple formulas is not possible, because the comparable high K-value makes it necessary also to include the off axis contributions. Off axis contributions are not only the result of the hybrid undulator – wiggler behavior of our insertion device but are also the result of multi particle effects of the beam which leads to a geometric spread of the beam (increase of emittance from scattering events, oscillations). The effect of the energy spread on the beams size is small because the location of the insertion devices have a small dispersion function.

PARAMETER		VALUE	PARAMETER		VALUE
Period length	cm	1.7	Alpha x		0.604
Periods		88	Alpha y		-0.836
K		1.78	Div x	rad	8.51E-5
Emittance x	mrad	6.91E-9	Div y	rad	9.98E-6
Emittance y	mrad	8.93E-11	Eta		-3.1E-3
Beam size x	m	9.49E-5	Theta x,y		0
Beam size y	m	1.17E-5	dTheta x		1.0E-3
Beta x	m	1.30	dTheta y		3.0E-4
Beta y	m	1.53			

***Table 2** – Input parameter for calculation with SPECTRA 10*

We selected the code SPECTRA10 [4] for the calculation of the synchrotron spectra because it also offers the possibility to include the beam parameters which influence the shape of the spectra through multi particle effects (*Table 2*). Besides the parameter of the undulator we also include the geometric aperture of the beamline. SPECTRA 10 integrates over the respective solid angle and we get the photon spectrum $d^2n/dtdE/E$ (f (E)) (blue line in *Figure 4*).

4.2. Input Spectrum

In the following we describe an algorithm that delivers energies for the primary photons with the same energy distribution as the original spectrum f (E) calculated in 4.1.
The first step is to integrate the spectrum and normalize the integral to 1. From our so calculated antiderivative function of the spectrum F (E) we need the inverse antiderivative function, to get the photon energy with the usage of a random number generator which draws equally distributed numbers from 0 to 1 (exclusive):

$$E_\gamma = ran[0,1) \cdot F^{-1} \tag{22}$$

Because we have no analytical expression for our antiderivative spectrum function we cannot give an analytical expression for its inverse function. We do it quasi graphically as show in *Figure 3*

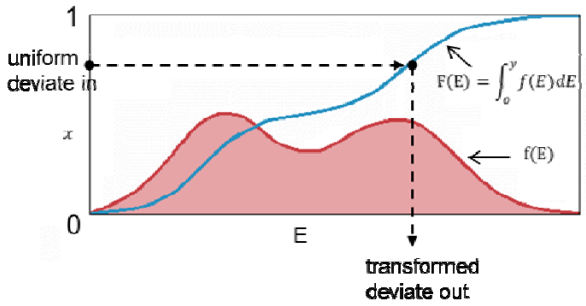

Figure 3 *–Sampling of synchrotron spectra*

We draw the random number [0, 1] and look for which energy the normalized antiderivative spectrum function F has the same value. The respective E is the energy for our next primary photon that is used next by FLUKA.
The results of this algorithm are shown together with the spectrum in *Figure 4*. The agreement of the drawn random energies (black) with the calculated spectrum (orange) is very good.

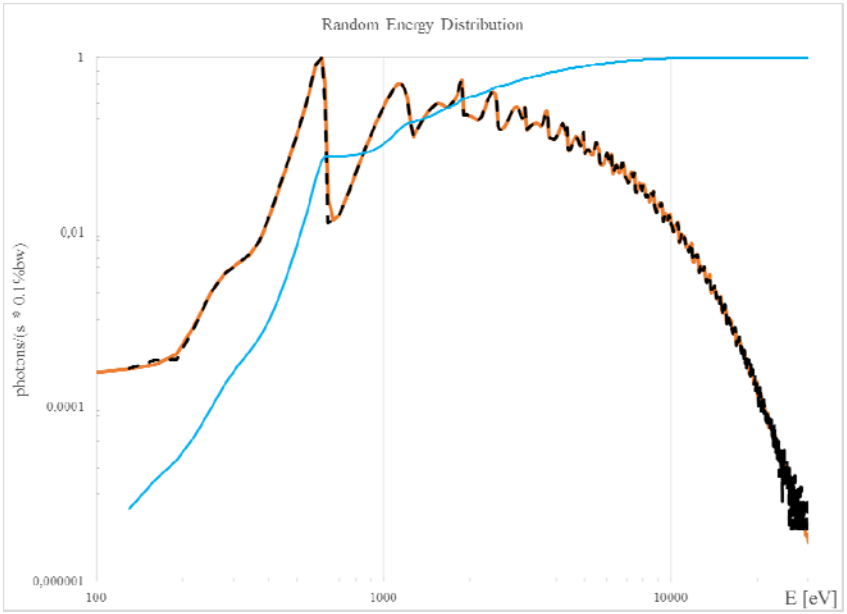

Figure 4 – *Spectrum of the U-17(orange = calculated spectrum, black = random energy, blue = integrated spectrum)*

If the properties of the primary particles are too complicated to be described with cards like BEAM or BEAMPOS Fluka offers the possibility to add a user written subroutine. The SOURCE-card activates the linked subroutine which samples from that spectrum so that the energy for every primary particle is calculated.
So in our case we included the algorithm in a substitute source.f and linked it to Fluka.
Although the subroutine can override definitions given in the input, the momentum or kinetic energy from the BEAM-card is meaningful by the reason that it defines the maximum energy.

5. Results and safety measures

5.1. Optics hutch

The safety measures consider to reach a dose limit for all accessible parts of the experimental hall of 1 mSv/a, and additionally a dose limit of less than 3 mSv/h for areas that are not interlock controlled exclusion areas is specified. To determine the measures of the shielding for the optics hutch where the beam conditioning elements are housed a simulation of the calculated synchrotron radiation inside the experimental hall gives the required information. As a conservative scenario we considered a scattering process at a closed slit near a bellow. In *Figure 5* the result of the simulation show the necessity of a shielded hutch in front of the shielding of the ring tunnel.

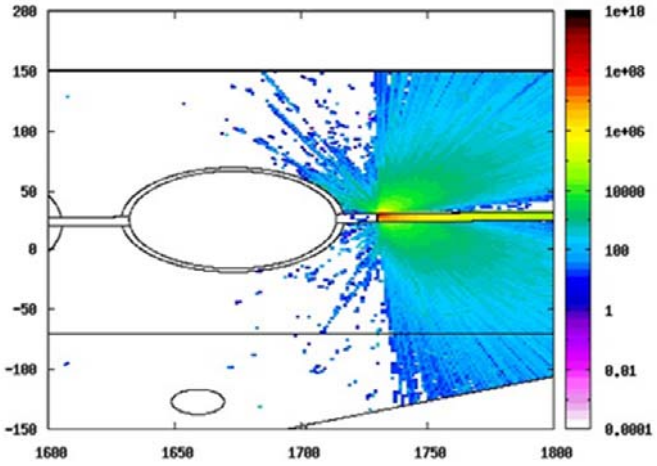

Figure 5 – *Dose distribution in optics hutch for a closed slit near a bellow in Sv/h*

The result of this scenario show that the requested dose limit for interlock free areas could not be held. To protect the accessible parts of the experimental hall the optics hutch contains of a lead sheet of 2 mm thickness sandwiched between 2 mm thick steel panels. To prevent a groundshine the floor and wall connections where realized as internal L-section coated with lead. To pay attention to the cable penetrations labyrinth chambers where used. The optics hutch is executed as an interlock controlled exclusion area so the entrance is forbidden if the beam shutter is open. In case of opening the door the beam shutter will close immediately to keep the radiation inside the tunnel. Before beam operation the hutch area must be searched and warned as restricted area due to radiation.

5.2. Pink hutch

One end station for the hard x-ray beam is the so called Pink experiment. The Pink-station has the option to use the direct undulator light which penetrates the experiment directly on air therefore DCM and GCh (grating chamber, installed behind DCM) has to clear the beam path. Due to the fact that the experiment will be part of our experimental hall and the intended dose rates of this area, the necessity of a hutch is completely obvious. To clarify that the beam in the Fluka simulation hits a target composed of water while the experiment is shielded by our hutch wall composed of the steel lead sandwich. The resulting dose rates inside the hutch are shown in *Figure 6*.

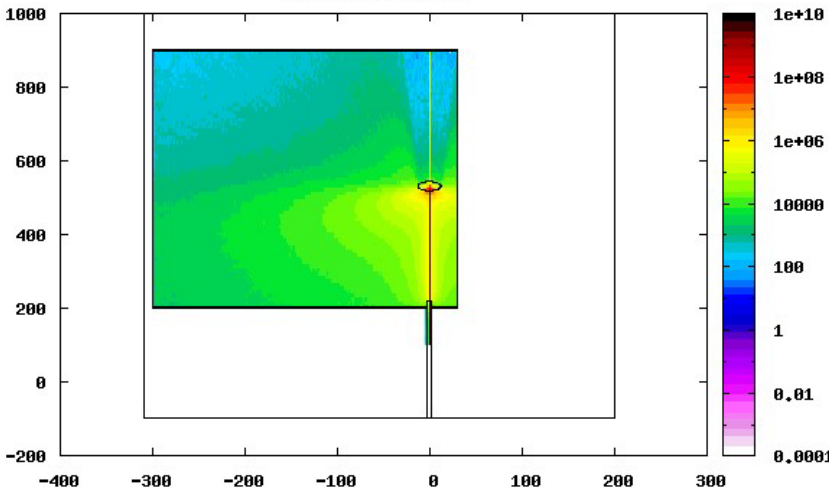

Figure 6 *- Dose distribution in Pink hutch at the experiment in Sv/h*

The dose rate could reach values of about $1 \cdot 10^7$ Sv/h so the shielding design requires a 3 mm lead sheet inside the hutch wall construction to assure the dose limit of the experimental hall. The Pink hutch will also be included into the interlock safety system with the same entrance requirements and safety measures as the optics hutch.

In *Figure 2* a third hutch is drawn for another experiment of the EMIL beamline inside the experimental hall, the PEEM (photo emission electron) hutch. This experiment will be delivered with soft x-ray only and no monochromator is inside so a lead shielding is not necessary for radiation safety reasons.

5.3. Simulation of Bremsstrahlung

The shielding wall of the ring tunnel consists in forward direction at the beamline angles of 1 m hematite concrete and a 5 cm lead screen. If there is no hutch outside the shielding wall these areas are interlock controlled exclusion areas caged with a fence. In the transversal direction the shielding wall consists of 1 m ordinary concrete or close to the front-ends of 0.8 m heavy concrete.
Due to the shielding measures a scenario which has to be taken into consideration is the impact of bremsstrahlung in forward direction at the beamline. Therefore we assume a beam loss at a steel tube of the straight section downstream the cryogenic in-vacuum undulator at an angle of 1 mrad. The resulting gamma dose is shown in *Figure 7*.

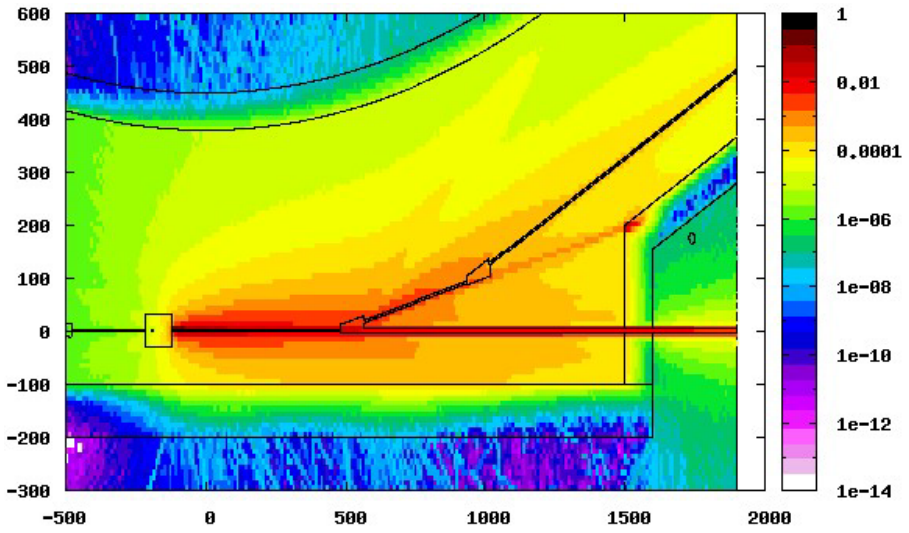

Figure 7 *- Gamma dose rate [Sv/h] - 10% loss of injected electrons in forward direction at 1 point in straight section*

The assumption of this scenario is a loss of 10% (a bigger average loss is not possible due to the top-up interlock conditions that controls the injection efficiency) of the injected electrons (1 nC/shot) per hour at only one spot in the storage ring. Our experience shows that most of the injected electrons get lost at the injection septum. A subsequent complete loss of the stored beam will probably not occur at only one spot, so the shown dose rates outside the shielding wall are very conservative scenarios. Furthermore the resulting dose rates show that the ratchet end wall reduces the gamma radiation in forward direction by five orders of magnitude (as well as the beam shutters) [10].

6. Summary

For the EMIL project at the Helmholtz-Zentrum Berlin two new x-ray beamlines were implemented at the storage ring BESSY II including a cryogenic in-vacuum undulator for the hard x-ray branch. To determine the shielding of the synchrotron radiation in the experimental hall we calculate the spectrum of the cryogenic undulator with SPECTRA 10. The energy distribution was used in a program code (self-written) that draws the random energy of primary photons with the same energy distribution as the original spectrum. This method was included into a source file and linked to Fluka to sample the spectrum and determine the thickness of the shielding walls of the different hutches. This new method allows for calculating the shielding of synchrotron radiation with Monte Carlo codes instead of analytic tools.

References

[1] R. Follath, M. Hävecker, G. Reichardt, K. Lips, J. Bahrdt, F. Schäfers, P. Schmid, “The Energy Material in Situ Lab (EMIL) at BESSY II”, J. Phys.: Conf. Ser. 425, 212003, 1-4 (2013)

[2] G. Battistoni, S. Muraro, P.R. Sala, F. Cerutti, A. Ferrari, S. Roesler, A. Fasso, J. Ranft, "The FLUKA code: Description and benchmarking", Proceedings of the Hadronic Shower Simulation Workshop 2006, Fermilab 6-8 September 2006, M. Albrow, R. Raja eds. AIP Conference Proceeding 896, 31-49, (2007)

[3] A. Fasso, A. Ferrari, J. Ranft, and P.R. Sala, "FLUKA: a multi-particle transport code" CERN-2005-10 (2005), INFN/TC_05/11, SLAC-R-773

[4] T. Tanaka and H. Kitamura, J. Synchrotron Radiat.8, 1221 (2001), SPECTRA is freely available from http://radiant.harima.riken.go.jp/spectra/index.html

[5] K. Ott, “Radiation Protection Issues of the Top-Up Operation of BESSY”, roc. 7th Intern. Workshop on Radiation Safety at Synchrotron Radiation Facilities (RADSYNCH13), BNL, New York, USA (2013)

[6] J. Bahrdt, H.-J. Bäcker, W. Frentrup, C. Rethfeldt, M. Scheer, B. Schulz, S. Gottschlich „A canted double undulator system with a wide energy range for EMIL“ IPAC 2015, Richmond, Virginia

[7] S. Hendel, F.Schäfers, R. Follath, M. Hävecker, G. Reichardt, M. Scheer, J. Bahrdt, K. Lips “Beamlines for the Energy Materials In-Situ Laboratory (EMIL) at BESSY-II” Journal of Synchrotron Radiation

[8] A. Hoffmann,” The Physics of Synchrotron Radiation”, Cambridge University Press, UK (2004)

[9] H. Wiedemann,” Particle Accelerator Physics”,Springer Verlag Berlin Germany, 3rd ed. (2007)

[10] K. Ott, Y. Bergmann, „FLUKA Calculations of Gamma Spectra at BESSY“, IPAC 2014, Dresden, Germany